Colloid Polym Sci (2010) 288:1167–1172
DOI 10.1007/s00396-010-2243-5

ORIGINAL CONTRIBUTION

Surface interaction forces mediated by poly(*N*-isopropylacrylamide) (PNIPAM) polymers: effects of concentration and temperature

Xiangjun Gong · Chi Wu · To Ngai

Received: 9 March 2010 / Revised: 5 May 2010 / Accepted: 7 May 2010 / Published online: 4 June 2010

Abstract Total internal reflection microscopy was used to directly measure the interaction potentials between a micron-sized silica sphere and a flat silica surface in the presence of a linear poly(*N*-isopropylacrylamide) (PNIPAM) aqueous solution. When the PNIPAM concentration was low, no discernible forces were detected. A further increase in PNIPAM concentration resulted in a long-range attraction which was likely due to a combined of the reduced electrostatic interaction between the silica particle and the flat surface after the polymer adsorption and polymer bridges formation. On the other hand, for a fixed PNIPAM concentration, the interaction potential profiles between the particle and flat surfae were once again characterized by attraction as temperature was incre
This attractive force can be explained in terms of the conformational changes of PNIPAM ch at the surfaes, which subsequently affected the polymer adsorption and enhanced the segment–segment interaction among the adsorbed polymer chains.

Keywords Total internal reflection microscopy (TIRM) · Surface force · Colloidal interaction · PNIPAM · Attractive force · Colloids

Electronic supplementary material The online version of this article (doi:10.1007/s00396-010-2243-5) contains supplementary material, which is available to authorized users.

X. Gong · C. Wu
Department of Physics, The Chinese University of Hong Kong, Shatin, NT, Hong Kong

C. Wu · T. Ngai (✉)
Department of Chemistry, The Chinese University of Hong Kong, Shatin, NT, Hong Kong
e-mail: tongai@cuhk.edu.hk

Introduction

The adsorption or grafting of polymers at an interface has long been of interest to researchers in severa branches of science, including chemistry, physics, and biology, as this technique can be to modi the surfae properties and tune the interaction forces [1]. Practically, the adsorption is relatively simple and widely used in industrial applications. Adsorbed layers are used to control adhesion and lubrication in minerals processing, wastewater treatment, and paper making, to name but a few important applications [2]. The adsorption of polymer is also widely used to control the stability of colloidal suspensions. If particle surfaces are fully covered with polymers, then the suspension can be stabilized because the steric repulsion that arises between the adsorbed layers of neighboring particles keeps the colloidal particles at a distant from one another. Under certain circumstances, however, long polymer chains adsorbed to one particle may stick to bare patches on the other, forming bridges and causing flocculation [3, 4]. Control the stability of colloidal particles also depends on whether the polymer chains are reversibly or irreversibly adsorbed and interactions of the polymer chains with substrates and solvent molecules [5–8].

During the past three decades, several studies have investigated the adsorption of polymers at the solid–liquid interface, the responses of the adsorbed layers to the changes of the environmental conditions, and the subsequent effect on the interaction forces between colloidal particles [9–12]. If the surfaces are saturated by adsorbed polymer chains, and the polymer between the surfaces can equilibrate with polymer in the bulk solution at all surface separation, as been suggested that the forces between two adsorbed polymer layers are attractive, mainly arising from polymer bridging [4, 7]. Another situation, the so-called constrained equilibrium, assumes that the amount of

adsorbed polymer is kept constant as two surfaces are brought toward each other and the rate constant for polymer adsorption is larger than that for desorption, i.e., the adsorbed polymer remains kinetically trapped between the two approaching surfaces. In such a case, and in good solvent conditions, de Gennes predicted that the interaction force between the two surfaces would be repulsive at all separation distances due to the unfavorable entropy of confinement [4]. In poor solvent conditions; however, he predicted that a long-range attraction would turn into a short-range repulsion if the particles are forced close enough to compress the adsorbed polymer layers [5–7]. The long-range attractive force may be attributable to a combination of bridging, depletion, or in poor solvents, intersegment attraction [7]. However, it is worth mentioning that the adsorption of polymers at the solid–liquid interface is somehow complicated. The absorption involves several distinctly different processes, including diffusion of the polymers in solution, molecular attachment onto the surface, and conformational relaxation of the polymer being adsorbed. Therefore, the experimental study of the polymer-mediated interactions between surfaces is difficult as adsorption conditions under which the contributions from the three processes can be unambiguously distinguished.

Many measurements on the interactions between surfaces bearing adsorbed polymers have been conducted by using techniques such as surface force apparatus (SFA) [13–19] and atomic force microscopy (AFM) [20–22]. These studies have confirmed the main features of the theoretically predicted interactions. For example, long-range attraction was detected in the case of mica surfaces bearing adsorbed polystyrene layers, which was enhanced when the solvent became poor [15, 16]. In a good solvent, on the other hand, the attractive force between two layers was weakened. However, it has been argued that both SFA and AFM methods are suitable for the study of large interaction energies, especially with a high degree of polymer layer compression and interpenetration. It may be questioned whether they are adequate for interactions which correspond to the Brownian collisions seen in actual colloids, where the detection of energy variations of the order of k_BT and beyond is required [8]. Recently, direct measurements of weak interactions have become possible with the improved sensitivity afforded by techniques such as optical tweezers [23, 24] and total internal reflection microscopy (TIRM) [25–28]. In particular, TIRM is an extremely sensitive noninvasive technique that has the ability to resolve the interaction distance and force between a free-moving colloid particle and a planar surface as close as 1 nm and as weak as a few femto-Newtons, respectively. TIRM is, therefore, admirably suited to the study of extremely weak and dynamic interactions that are most relevant to the properties of colloidal particles stabilized with polymer layers. It also offers an easy way to vary the ambient conditions, such as the polymer concentration, ionic strength, and temperature [25].

In this study, TIRM was used to directly measure the interactions between a 5.0-μm silica spherical particle and a hydrophilic silica surface, when both surfaces physically absorbed the thermo-responsive polymer, poly(*N*-isopropylacrylamide) (PNIPAM). It has been reported that PNIPAM exhibits a lower critical solution temperature (LCST) of ~32 °C in aqueous solution, and the effects of temperature on the polymer structure and hydration are well documented in the literatures [29–31]. When PNIPAM chains are adsorbed or grafted to surfaces, the surface properties can be reversibly altered by changing the temperature above and below the LCST [32–34]. It is interesting to note that the temperature-induced change of PNIPAM conformation or hydration has recently been correlated to substantial changes in the adhesion of biological cells and proteins [35]. Therefore, there is a clear need to control and characterize the architecture of PNIPAM coatings and to gain improved understanding of how the microstructure affects interactions with biomolecules. This is the motivation for the present work. We directly measure the interfacial interactions between PNIPAM-coated colloidal particle and flat surface above and below the LCST. In contrast to the conventional approaches such as studying the adsorption isotherms or measuring total thickness of the adsorption layer, the direct force measurement utilized here is a robust approach which provides valuable insights into the polymer-mediated interaction between two surfaces.

Experimental part

Materials The synthesis and fractionation of PNIPAM have been detailed elsewhere [36]. The weight average molar mass (M_w), the polydispersity index (M_w/M_n), and the radius of gyration (R_g) of the PNIPAM fraction used in present study are 4.0×10^6 g/mol, 1.8, and 105 nm, respectively. The average hydrodynamic radius (R_h) of the PNIPAM at room temperature is around 75 nm, as determined by dynamic laser light scattering (DLS). Hydrophilic silica particles with a diameter of ~5.0 μm (CV ~10%) were purchased from Polysciences Inc., and used without further treatment. Silica microscopy slides (BK-7 glass) were obtained from Fischer Scientific Co. The NaCl (GR from BDH) was heated at ~200 °C for 2 days to remove organic impurities. Water was purified with an inverse osmosis filtration (Nano Pure, Barnstead) until its resistivity reached 18.2 MΩ·cm at 20 °C and was then filtered with a Milipore PTFE 0.45-μm hydrophilic filter.

Physical measurements A laser light scattering (LLS) spectrometer equipped with an ALV-5000 multi-τ digital time

correlator and a He-Ne laser (output power=28 mW at λ_0= 632.8 nm) was used to characterize the PNIPAM chains. M_w and R_g of PNIPAM chains in a dilute solution was obtained from the angular dependence of the excess absolute scattering intensity, known as the Rayleigh ratio R_{vv} (q). The intensity–intensity time correlation function $G^{(2)}(\tau)$ was measured at the scattering angle 17.5°. The Laplace inversion of $G^{(2)}(\tau)$ can lead to a line-width distribution $G(\Gamma)$, which was further converted to a translational diffusive coefficient distribution $G(D)$ by $\Gamma=Dq^2$ or a hydrodynamic radius distribution $f(R_h)$ by use of the Stokes–Einstein eq.,$R_h = k_BT/6\pi\eta D$, where η, k_B, and T are the solvent viscosity, the Boltzmann constant, and the absolute temperature, respectively. The details of the LLS theory can be found elsewhere [37, 38]. The zeta potential (ζ) of the silica particles and PNIPAM-coated particles was measured using a commercial zeta-potential spectrometer (ZetaPlus, Brookhaven).

TIRM TIRM is a technique which measures the mean potential energy of interactions between a free-moving spherical particle and a flat plate. This technique has been described elsewhere [25, 39, 40]. Typically, in TIRM force measurement, a very diluted (the stock solution was diluted down to a concentration of ~10^{-7}g/mL) silica dispersion was initially filled into a carbonized PTFE frame sandwiched between two silica microscopy slides. The slides were first cleaned by ultrasonication for 15 min in ethanol and then blown to dry by highly pure nitrogen. The dried slides were dipped in 5% hydrofluoric acid (HF) solution and then rinsed copiously with D.I. water [41, 42]. The treated slides were then stored in ethanol. Before the measurements, the slides were further treated by ultraviolet (UV)-ozone plasma cleaner (Harrick Sci. Corp.) to ensure that the silica surface was fully hydroxylated to promote adsorption of PNIPAM through hydrogen bonding [43, 44].

A silica particle of average brightness was selected and hold in place with optical tweezers by a solid-state Nd:YAG laser (output=300 mW at wavelength=532 nm), while the rest of the silica particles were flushed from the TIRM cell with NaCl solution. Once the excess particles were pushed through the sample cell, the interaction between the single free-moving silica particle and bare glass surface in 0.2 mM NaCl solution was recorded. PNIPAM solution ($C = 1.0 \times 10^{-5}$g/mL) in 0.2 mM NaCl was then introduced in the sample cell to replace the pure NaCl solution by a flex tubing pump (Master Flex), while the silica particle was trapped in place by tweezers. Prior to measuring potential in the presence of PNIPAM chains, the silica particle and the glass slides were subjected to 1 h of contact with PNIPAM solution. Previous studies [32, 45, 46] have shown that long PNIPAM chains are irreversibly absorbed to the silica surface through the hydrogen bonding between the carbonyl groups of the PNIPAM and the silanol groups on the silica surface. The potential profiles between the silica particle and flat surface in the PNIPAM aqueous solution were first obtained at room temperature. After that, the temperature of the solution was then gradually increased. A pair of Peltier modules (Shenzhen GuangTongYuan Industry) each mounted with thermal radiators was used as a built-in thermostat to regulate the temperature of the sample cell. The temperature in the range 18.0–45.0 °C could be achieved with long term stability of ±0.1 °C.

Results and discussion

Figure 1 shows the PNIPAM concentration dependent on the interaction profiles between the silica particle and flat surface in NaCl aqueous solution at temperature of 25 °C. If no PNIPAM presents in the solution, the total interaction potential of the negatively charged silica particle at height h above the negatively charged flat surface is given by electrostatic double-layer repulsion and gravity and can be described as [25, 47, 48]:

$$\frac{\Phi(h)}{k_BT} = Be^{-\kappa h} + \frac{G}{k_BT}h \quad (1)$$

where the amplitude of the electrostatic interaction B depends on the surface charges of the particle and the glass surface, κ^{-1} is the Debye screening length of the solvent, and G is the weight of the particle. The solid line in the Fig. 1 shows that the measured potential is well described by Eq. 1, with the fit yielding a value of $\kappa^{-1} \approx 26 \pm 1$nm for the Debye length that is in agreement with the theoretical values as calculated with the used electrolyte concentration [47, 48]. After pumping a low concentration (1.0×10^{-5}g/mL) of the PNIPAM solution through the sample cell and waiting for ~1 h at 25 °C, the interaction potential shifted slightly away (~10 nm) from the surface, indicating that the addition of PNIPAM induces a repulsive

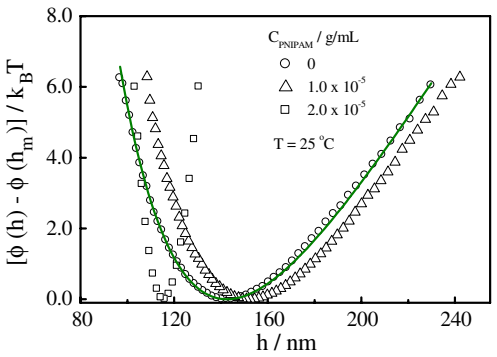

Fig. 1 Potential energy profiles measured between a 5.0-μm silica particle and a flat glass surface in various concentrations of PNIPAM aqueous solutions at 25 °C. The *solid line* shows that the measured data are well fitted by Eq. 1

force. The likely reason for such shifting may be due to the so-called constrained equilibrium in this experiment. Considering that the amount of PNIPAM is constant as two surfaces are brought toward each other and the rate constant for polymer adsorption is larger than that for desorption, the adsorbed PNIPAM chains therefore will be kinetically trapped between the two approaching surfaces. In such a case, and in good solvent conditions, the interaction force between the two surfaces would be repulsive because of the unfavorable entropy of confinement. However, the measured force is very weak and long range (around 150 nm) so that further studies and comparison with theoretical works are needed to clarify this point. When the PNIPAM concentration is further increased, Fig. 1 shows that the interaction potential is much narrower and steeper, and the particle-surface distance is reduced to ~120 nm with a PNIPAM concentration of 2×10^{-5} g/ml, indicating that an attractive force is induced pushing the particle closer to the flat surface.

Previous studies have shown that long PNIPAM chains are irreversibly absorbed to the silica surface within several minutes through the hydrogen bonding between the carbonyl groups of the PNIPAM and the silanol groups on the silica surface [45, 46]. On the other hand, as determined from DLS, the hydrodynamic radius (R_h) of the free PNIPAM chain at 25°C was ~75 nm. That means twice the R_h is approximately equal to or larger than the gap between the particle and flat surface. Therefore, one may wonder whether the measured attractive force is either due to the alternation of the electrostatic interaction between two surfaces after the absorption of PNIPAM chains or to the polymer bridging. After mixing silica particle with 2×10^{-5} g/mL PNIPAM polymer overnight, zeta potential measurements show that the bare silica particle with a potential of −65 mV decreases to −10 mV when PNIPAM chains are absorbed onto surface. The electrostatic repulsion between the silica particle and flat surface is expected to be reduced. We, therefore, suggest that the measured attractive force likely caused by a combination of the alternation of surface properties and polymer bridging. We infer that the adsorption PNIPAM chains onto the surfaces reduce the electrostatic interaction between the two surfaces so that the particle moves closer to the flat surfaces, which in turn facilitates bridging. The steric repulsion due to the compression of adsorbed chains may play a minor role. It is interesting to note that after the measurement, pure 0.2 mM NaCl solution was subsequently pumped to rinse the sample cell for 3 h. The interaction potential remains the same, indicating that rinsing the sample cell cannot completely desorbed the adsorbed PNIPAM chains from both particle and flat surface or disruption the polymer bridges.

As mentioned above, PNIPAM is a thermally sensitive polymer which is insoluble and undergoes a conformational change above its LCST of ~32°C [29–31]. Below the LCST, the polymer chains swell in water, while above LCST, the solvent quality changes and the polymer segments are thought to become more hydrophobic. Therefore, it would be interesting to explore how the temperature-induced conformation change of PNIPAM affects the adsorption process as well as whether different conformations of the adsorbed PNIPAM affect the interfacial

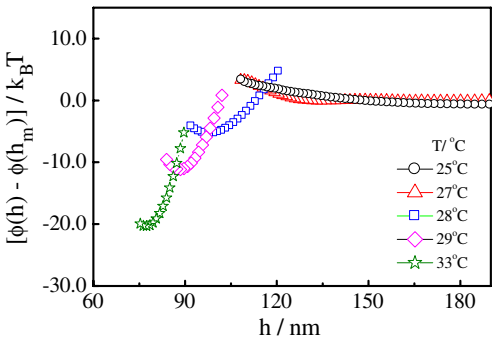

Fig. 3 Temperature dependence of the net potential energy profiles measured between a 5.0-μm silica particle and a flat glass surface with the presence of 1.0×10^{-5} g/mL PNIPAM aqueous solution after subtracting gravity and double layer repulsion from the bare silica particle and flat surface

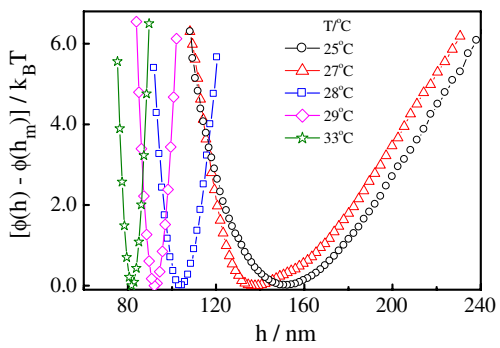

Fig. 2 Temperature dependence of the potential energy profiles measured between a 5.0-μm silica particle and a flat glass surface with the presence of 1.0×10^{-5} g/mL PNIPAM chains in 0.2 mM NaCl aqueous solution

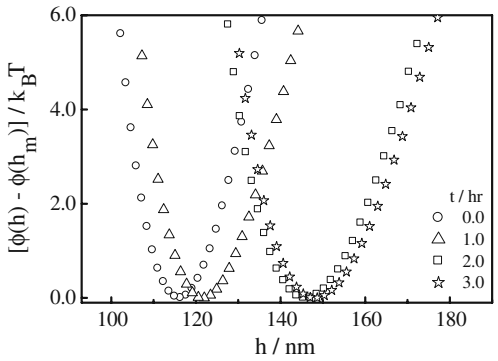

Fig. 4 Time dependence on the interaction potentials between a 5.0-μm silica particle and a flat glass surface when the solution temperature was further decreased to 20°C after the temperature-increase process

potentials between the probe particle and the flat substrate. Figure 2 shows the temperature dependence of the interaction profiles between the silica particle and flat surface in the presence of 1.0×10^{-5} g/mL PNIPAM solution, where each interaction potential was obtained at least 1 h after the solution reached the desired temperature. As can be seen from Fig. 2, when the temperature was increased, the measured interaction potentials became narrower and shifted closer to the surface, indicating that the increase of temperature leads to an attraction. Note that the interaction potentials between the silica particle and the surface in a 0.2-mM NaCl aqueous solution without the presence of PNIPAM have no any change over the entire temperature range we investigated. Because the consecutive potentials are measured with the same silica particle and same surface at different temperatures, we have subtracted the contributions of particle–surface interaction potential in the absence of PNIPAM at 25 °C from all potentials in order to isolate the effects of adsorbed polymer's response to the solution temperature.

The results of this subtraction are depicted in Fig. 3. At temperatures below 28 °C, a weak repulsive force was detected. The origin of this weak and long-range repulsion is likely due to the steric interaction when the extended PNIPAM chains between the surfaces are compressed in the confined region. However, as temperature continuously increased, in particular above 28 °C, the interaction potential between two surfaces tuned from the long-range repulsion to attraction. Some previous studies reported that for PNIPAM chain adsorbed to a solid surface, the "coil-to-globule" transition occurred at ~29 °C which is about 3° lower than the LCST of the same PNIPAM chains free in bulk solution [49]. We thereby conjecture that by rising the temperature above 28 °C, around the LCST of PNIPAM at the interface, may result in differences in the adsorption kinetics of the polymer chains and consequently results in the long-range attraction between the two surfaces. At higher temperatures, the adsorbed PNIPAM chains are collapsed and less stretched so that the interactions between PNIPAM chains and water are lower. In such a case, more free PNIPAM chains can be adsorbed on the surface even under the same polymer solution to form more bridges. In addition, as the solvent quality deteriorates at higher temperatures, the segment–segment interactions among the adsorbed PNIPAM chains between two surfaces will also be enhanced, leading to a strong attraction.

After completed the measurement at high temperatures, the temperature inside the sample cell was decreased to 20 °C. It is expected that at such a lower temperature, water is a much better solvent for the PNIPAM chains and will be more favorable for the polymer desorption, if it exists. Figure 4 shows that the interaction potentials shifted away from the surface but the silica particle cannot escape to be freely moving during the entire measurement. This confirms the formation of polymer bridges between the two surfaces. The gradual movement of the particle away from the surface may mainly due to the swelling of the compressed polymer chains at a lower temperature. The irreversible adsorption and bridging of long PNIPAM between the two silica surfaces can be attributed to the nature of adsorption and desorption of polymer chains. In other words, for each PNIPAM chain adsorbed between two surfaces, there would be more than one adsorption "point" along the chain; and for each adsorption "point," there exists a dynamic equilibrium between the adsorption and desorption, but the desorption of the entire polymer chain from the surface requires not only a simultaneous releasing of all the adsorbing "points" but also an immediate diffusion away from the surface. Therefore, it is much more difficult for an adsorbed PNIPAM chain to become free again after its adsorption on the surfaces [49, 50].

Conclusions

Using TIRM, we have directly measured the interaction potentials between a silica sphere and a flat silica substrate in the presence of a thermally sensitive PNIPAM solution. We found that the interaction potentials between the surfaces showed responsiveness to both concentration and temperature. For a fixed temperature, the increase of polymer concentration resulted in a long-range attraction due to the reduced electrostatic repulsion between two surfaces and formation of polymer bridges. On the other hand, for a fixed PNIPAM concentration, increased temperature caused a conformational change of the interfacial adsorbed PNIPAM chains which not only facilitated more bridging due to additional adsorbed chains but also enhanced segment–segment interaction among adsorbed polymer chains. Our findings offer a novel approach for the design of temperature controllable polymer layers with respect to binding and release of cell and protein molecules.

Acknowledgement This study was financially supported by Hong Kong Special Administration Region Earmarked Project grant (CUHK402506, 2160291) and by a Direct Grant for Research 2008/09 from the Chinese University of Hong Kong (CUHK 2060371).

References

1. Fleer GJ, Stuart MAC, Scheutjens JMHM, Cosgrove T, Vincent B (1993) Polymers at interfaces, 1st edn. Chapman and Hall, Cambridge
2. Israelachvili JN (1992) Intermolecular and surface forces, 2nd edn. Academic, New York
3. Swenson J, Smalley MV, Hatharasinghe HLM (1998) Mechanism and strength of polymer bridging flocculation. Phys Rev Lett 81:5840–5843
4. de Gennes PG (1982) Polymers at an interface. 2. interaction between two plates carrying adsorbed polymer layers. Macromolecules 15:492–500

5. Klein J, Pincus PA (1982) Interaction between surfaces with adsorbed polymers: poor solvents. Macromolecules 15:1129–1135
6. Klein J, Rossi J (1998) Analysis of the experimental implications of the scaling theory of polymer adsorption. Macromolecules 31:1979–1988
7. Scheutjens JMHM, Fleer GJ (1985) Interaction between two adsorbed polymer layers. Macromolecules 18:1882–1900
8. Kleshchanok D, Tuinier R, Lang PR (2008) Direct measurements of polymer-induced forces. J Phys: Condens Matter 20(7):073101
9. Yamamoto S, Ejaz M, Tsujii Y, Matsumoto M, Fukuda T (2000) Surface interaction forces of well-defined, high-density polymer brushes studied by atomic force microscopy. 1. effect of chain length. Macromolecules 33:5602–5607
10. Wang J, Butt HJ (2008) Forces between thiolate-modified gold surfaces in a melt of end-functionalized polymers. J Phys Chem B 112:2001–2007
11. Notley SM, Biggs S, Craig VSJ (2003) Application of a dynamic atomic force microscope for the measurement of lubrication forces and hydrodynamic thickness between surfaces bearing adsorbed polyelectrolyte layers. Macromolecules 36:2903–2906
12. Claesson PM, Poptoshev E, Blomberg E, Dedinaite A (2005) Polyelectrolyte-mediated surface interactions. Adv Colloid Interface Sci 114–115:173–187
13. Klein J (1980) Forces between mica surfaces bearing layers of adsorbed polystyrene in cyclohexane. Nature 288:248–250
14. Klein J, Luckham PF (1984) Long-range attractive forces between two mica surfaces in an aqueous polymer solution. Nature 308:836–837
15. Klein J, Luckham PF (1984) Forces between two adsorbed poly (ethylene oxide) layers in a good aqueous solvent in the range 0–150 nm. Macromolecules 17:1041–1048
16. Granick S, Patel S, Tirrell M (1986) Direct measurement of intermolecular forces between a polymer layer and mica. J Chem Phys 85:5370–5371
17. Hadziioannou G, Patel S, Granick S, Tirrell M (1986) Forces between surfaces of block copolymers adsorbed on mica. J Am Chem Soc 108:2869–2876
18. Hu HW, Granick S (1990) Universal and system-specific features of surface forces between adsorbed polystyrene in a near-Θ solvent. Macromolecules 23:613–623
19. Ruths M, Israelachvili JN, Ploehn HJ (1997) Effects of time and compression on the interactions of adsorbed polystyrene layers in a near-θ solvent. Macromolecules 30:3329–3339
20. Biggs S (1995) Steric and bridging forces between surfaces bearing adsorbed polymer: an atomic force microscopy study. Langmuir 11:156–162
21. Braithwaite GJC, Howe A, Luckham PF (1996) Interactions between poly(ethylene oxide) layers adsorbed to glass surfaces probed by using a modified atomic force microscope. Langmuir 12:4224–4237
22. Kelley TW, Schorr PA, Johnson KD, Tirrel M, Frisbie CD (1998) Direct force measurements at polymer brush surfaces by atomic force microscopy. Macromolecules 31:4297–4300
23. Verma R, Crocker JC, Lubensky TC, Yodh AG (2000) Attractions between hard colloidal spheres in semiflexible polymer solutions. Macromolecules 33:177–186
24. Owen RJ, Crocker JC, Verma R, Yodh AG (2001) Measurement of long-range steric repulsions between microspheres due to an adsorbed polymer. Phys Rev E 64:011401
25. Prieve DC (1999) Measurement of colloidal forces with TIRM. Adv Colloid Interface Sci 82:93–125
26. Bevan MA, Prieve DC (2000) Forces and hydrodynamic interactions between polystyrene surfaces with adsorbed PEO −PPO−PEO. Langmuir 16:9274–9281
27. Fernandes GE, Bevan MA (2007) Equivalent temperature and specific ion effects in macromolecule-coated colloid interactions. Langmuir 23:1500–1506
28. Kleshchanok D, Lang PR (2007) Steric repulsion by adsorbed polymer layers studied with total internal reflection microscopy. Langmuir 23:4332–4339
29. Wu C (1998) A comparison between the 'coil-to-globule' transition of linear chains and the volume phase transition of spherical microgels. Polymer 39:4609–4619
30. Liu GM, Zhang GZ (2005) Collapse and swelling of thermally sensitive poly(*N*-isopropylacrylamide) brushes monitored with a quartz crystal microbalance. J Phys Chem B 109:743–747
31. Liu GM, Cheng H, Yan L, Zhang GZ (2005) Study of the kinetics of the pancake-to-brush transition of poly(*N*-isopropylacrylamide) chains. J Phys Chem B 109:22603–22607
32. Schönhoff M, Larsson A, Welzel PB, Kuckling D (2002) Thermoreversible polymers adsorbed to colloidal silica: A ^{1}H NMR and DSC study of the phase transition in confined geometry. J Phys Chem B 106:7800–7808
33. Goodman D, Kizhakkedathu JN, Brooks DE (2004) Attractive bridging interactions in dense polymer brushes in good solvent measured by atomic force microscopy. Langmuir 20:2333–2340
34. Callewaert M, Grandfils C, Boulange-Petermann L, Rouxhet PG (2004) Adsorption of poly(*N*-isopropylacrylamide) on glass substrata. J Colloid Interface Sci 276:299–305
35. Song SY, Choi HG, Hong JW, Kim BW, Sim SJ, Yoon HC (2008) Selective antigen–antibody recognition on SPR sensor based on the heat-sensitive conformational change of poly(*N*-isopropylacrylamide). Colloids Surf A Physicochem Eng Aspects 313–314:504–508
36. Zhou SQ, Fan SY, Au-yeung SCF, Wu C (1995) Light-scattering studies of poly(*N*-isopropylacrylamide) in tetrahydrofuran and aqueous solution. Polymer 36:1341–1346
37. Berne B, Pecora R (1976) Dynamic light scattering. Plenum, New York
38. Chu B (1991) Laser light scattering, 2nd edn. Academic, New York
39. Prieve DC, Frej NA (1990) Total tnternal reflection microscopy: a quantitative tool for the measurement of colloidal forces. Langmuir 6:396–403
40. Bike SG (2000) Measuring colloidal forces using evanescent wave scattering. Curr Opin Colloid Interface Sci 5:144–150
41. Frantz P, Granick S (1992) Surface preparation of silicon for polymer adsorption studies. Langmuir 8:1176–1182
42. Sukhishvili SA, Granick S (1998) Polyelectrolyte adsorption onto an initially-bare solid surface of opposite electrical charge. J Chem Phys 109:6861–6869
43. Johnson HE, Granick S (1992) New mechanism of nonequilibrium polymer adsorption. Science 255:966–968
44. Frantz P, Granick S (1995) Infrared dichroism, chain flattening, and the bound fraction histogram in adsorbed poly(methyl methacrylate) layers. Macromolecules 28:6915–6925
45. Walldal C, Wall S (2000) Coil-to-globule-type transition of poly(*N* -isopropylacrylamide) adsorbed on colloidal silica particles. Colloid Polym Sci 278:936–945
46. Notley SM (2008) Conformation of adsorbed layers of polyNIPAM on silica in a binary Solvent. J Phys Chem B 112:12650–12655
47. Jin F, Gong XJ, Ye J, Ngai T (2008) Direct measurement of the nanobubble-induced weak depletion attraction between a spherical particle and a flat surface in an aqueous solution. Soft Matter 4:968–971
48. Ngai T, Xing XC, Jin F (2008) Depletion attraction between a polystyrene particle and a hydrophilic surface in a pluronic aqueous solution. Langmuir 24:13912–13917
49. Gao J, Wu C (1997) The "Coil-to-Globule" transition of poly(*N*-isopropylacrylamide) on the surface of a surfactant-free polystyrene nanoparticle. Macromolecules 30:6873–6876
50. Hu TJ, Gao J, Wu C, Auweter H, Iden R (2002) Temperature induced hydrophobic adsorption and desorption of linear polymer chains on surfactant-free latex nanoparticles. J Phys Chem B 106:9815–9819